OPEN ACCESS

Original research

The butterfly effect: improving brain cone-beam CT image artifacts for stroke assessment using a novel dual-axis trajectory

Nicole Mariantonia Cancelliere [ID],[1,2] Eric Hummel,[3] Fred van Nijnatten [ID],[3] Peter van de Haar,[3] Paul Withagen,[3] Marijke van Vlimmeren,[3] Bertan Hallacoglu,[3] Ronit Agid,[4] Patrick Nicholson,[4] Vitor Mendes Pereira[1,2]

[1]Departments of Neurosurgery and Medical Imaging, St Michael's Hospital, Toronto, Ontario, Canada
[2]Keenan Research Centre, Li Ka Shing Knowledge Institute, Toronto, Ontario, Canada
[3]Image Guided Therapy, Philips Healthcare, Best, Noord-Brabant, The Netherlands
[4]Joint Department of Medical Imaging, Toronto Western Hospital, Toronto, Ontario, Canada

Correspondence to
Nicole Mariantonia Cancelliere, Departments of Neurosurgery and Medical Imaging, St Michael's Hospital, Toronto, ON M5B 1W8, Canada; nicole.cancelliere@unityhealth.to

ABSTRACT

Background Cone-beam computed tomography (CBCT) imaging of the brain can be performed in the angiography suite to support various neurovascular procedures. Relying on CBCT brain imaging solely, however, still lacks full diagnostic confidence due to the inferior image quality compared with CT and various imaging artifacts that persist even with modern CBCT.

Objective To perform a detailed evaluation of image artifact improvement using a new CBCT protocol which implements a novel dual-axis 'butterfly' trajectory.

Methods Our study included 94 scans from 47 patients who received CBCT imaging for assessment of either ischemia or hemorrhage during a neurovascular procedure. Both a traditional uni-axis 'circular' and novel dual-axis 'butterfly' protocol were performed on each patient (same-patient control). Each brain scan was divided into six regions and scored out of 3 based on six artifacts originating from various physics-based and patient-based sources.

Results The dual-axis trajectory produces CBCT images with significantly fewer image artifacts than the traditional circular scan (whole brain average artifact score, AS: 0.20 vs 0.33), with the greatest improvement in bone beam hardening (AS: 0.13 vs 0.78) and cone-beam artifacts (AS: 0.04 vs 0.55).

Conclusions Recent developments in CBCT imaging protocols have significantly improved image artifacts, which has improved diagnostic confidence for stroke and supports a direct-to-angiography suite transfer approach for patients with acute ischemic stroke.

Key messages

⇒ Cone-beam CT scans with a circular trajectory are subject to various artifacts, including cone beam, bone beam hardening, and metallic artifacts.

⇒ By modifying the X-ray tube trajectory to include caudal and cranial angulations, dual-axis cone-beam CT scans improve cone-beam and beam hardening artifacts.

⇒ These image quality enhancements improve assessment of hemorrhagic and ischemic stroke lesions, particularly in the upper supratentorial and posterior fossa of the brain.

Ideally CBCT could be used for treatment triage of patients with AIS and hopefully used to bypass the need for conventional CT to bring patients directly to the angiography suite for mechanical thrombectomy. Various groups have shown that a direct-to-angiosuite transfer approach can reduce door-to-puncture times by 30 min or more,[6] which may improve outcomes for patients with AIS.[7] Full confidence in relying solely on CBCT for stroke imaging workup is lacking, however, as current CBCT image quality is inferior in comparison with CT.[1]

Despite recent protocol improvements to incorporate advanced reconstruction algorithms,[5 8 9] CBCT image quality is still limited by various image artifacts, which contribute to a loss of anatomical information.[1 3 5] Image artifacts, such as streaks, image distortion, or contrast inhomogeneity, can arise from various physics-based or patient-based sources like beam hardening or metallic artifacts.[10 11] In an attempt to improve some of these artifacts, we have developed a CBCT protocol with a novel dual-axis trajectory that includes both caudal and cranial angulations along the tube rotation and a new 3D reconstruction method. The purpose of this study was to perform a detailed evaluation of image artifact improvements for this new dual-axis scan.

METHODS
Patient selection
All patients with acute stroke presenting at, or transferred to, our primary stroke center and

INTRODUCTION
Acquiring cone-beam computed tomography (CBCT) imaging of the brain in the angiography suite has great diagnostic value for neurointerventional procedures. Studies have shown that CBCT imaging is reliable for hemorrhage characterization,[1 2] which can be of great value during long or complex procedures where bleeding risks are high, such as arteriovenous malformation or fistula embolizations. Detection of ischemic lesions using CBCT is also possible,[3–5] which has supported a sparked interest towards using this technology in patients presenting with acute ischemic stroke (AIS).

BMJ

SNIS

selected for mechanical embolectomy were prospectively considered in this study. This study was approved by our institutional research and ethics board (ID # 16–5036). Consent for participation was provided by either the patient or a substitute decision-maker. Only patients who received both a circular and dual-axis scan were included in our study. Patients who underwent only one CBCT scan were excluded from the analysis as it was performed using an intrapatient control (paired-data analysis).

Advanced cone-beam CT image acquisition protocols

At the beginning of the endovascular procedure, two unique non-contrast flat-panel detector CBCT acquisition protocols were performed: a 10.4 s circular scan and an 8 s dual-axis (DA) 'butterfly' scan. Tuy[12] proves that a cone-beam acquisition on a circular trajectory does not generate sufficient information to allow for an exact reconstruction. Any attempt to heuristically reconstruct the incomplete dataset will necessarily have artifacts, so called *cone-beam artifacts*. The butterfly DA trajectory is designed to be complete with respect to Tuy's completeness condition, such that it allows for exact reconstruction, and should thus not exhibit cone-beam artifacts. The trajectory employs a 200 degree circular right to left rotation using the 'propeller' motion of the C-arm, with a simultaneous sinusoidal 'roll' motion of 15 degrees amplitude in the caudal to cranial angulation (online supplemental video 1). A similar trajectory was proposed by Schomberg.[13]

Both scans use a 120 kV peak potential applied to the X-ray tube with a 200 degree rotation and are acquired at 60 frames per second; however, the circular scan is acquired over 10.4 s and produces 620 projection images with a CT Dose Index of 45 mGy, whereas the DA scan is only 8 s long and produces 480 images with a corresponding dose of 45 mGy.[14 15]

Both scans were sequentially acquired in a random order using a biplane neuroangiography X-ray system (Allura Clarity FD20/15; Philips Healthcare, Best, the Netherlands), equipped with a caesium iodide–amorphous silicon flat-panel detector (detector sensor area=30 x 40 cm; matrix=2586 x 1904 pixels). The X-ray tube settings were as follows: voltage=120 kV, focal spot=0.7 mm, and copper filter=0.4 mm.

Both scans include the same preprocessing steps of the projection images beyond those of the standard commercially available CBCT scan, which include offset correction, gain correction, scatter correction, and water beam-hardening correction. 3D reconstruction of both protocols is obtained using Schomberg's method,[16] with an additional two-pass bone beam hardening correction applied as is commonly done in CT reconstruction.[17–19] Images were reconstructed in a volume of 252 mm³, subdivided in 384³ equal-sized voxels.

Motion artifact postprocessing algorithm

Motion artifacts are common on CBCT scans with longer acquisition times, such as those being used in our study (>8 s). Therefore, in order to minimize these, which may mimic other types of artifacts such as bone beam hardening, all scans in our study were postprocessed using a previously described motion-artifact correction algorithm (Cancelliere *et al*, accepted *JNIS*). This has been shown to effectively improve motion artifacts in 91% of CBCT scans. Although very effective, patient motion was still included in our artifact analysis to account for the remaining artifacts that might not be completely improved.
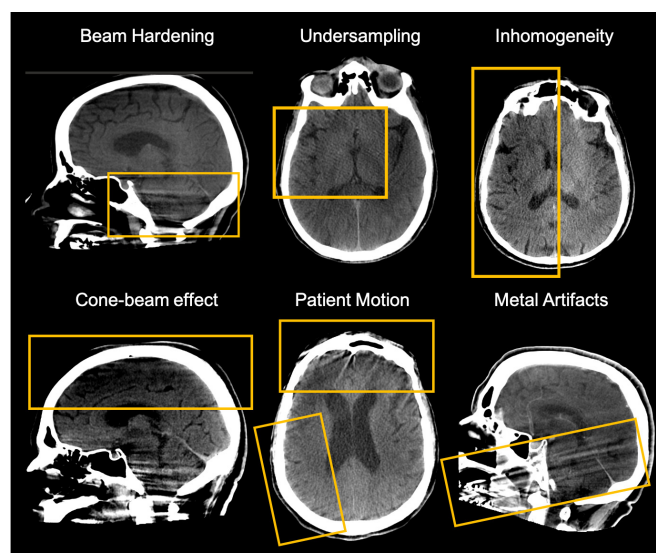

Figure 1 Cone-beam CT (CBCT) image artifact assessment scale: (1) beam hardening: streaks caused by dense bones (i.e., skull); (2) undersampling: view or ray aliasing, fine stripes radiating from the edges of dense structures; (3) inhomogeneity: darkness on one side of the brain vs the other; (4) cone-beam effect: dark bands at top and/or bottom of image; (5) patient motion: misregistration artifacts, blurry image or appearance of shading or streaking. (6) metallic artifacts: severe streaking artifacts radiating from a metallic object (i.e., dental fillings, surgical clips, or stents).

Image artifact analysis

Images were reviewed to determine six types of artifacts most prevalent in CBCT images: (1) beam hardening, (2) undersampling, (3) inhomogeneity, (4) cone-beam, (5) metallic, and (6) patient motion artifacts. The definitions and examples of these artifacts are outlined in figure 1 and were used in the analysis of our dataset. All scans were divided into six brain regions: left and right hemisphere of the upper supratentorial region (above the thalamus); left and right hemisphere of the lower supratentorial regions (below the thalamus) as well as the left and right sides of the posterior fossa. Two neuroradiology imaging experts assigned each of the six brain regions a score between 0 to 3 (none to severe) for each of the six types of artifacts, for a total of 36 scores per patient scan. A score of 1 was given if some mild artifacts were present, but image quality was deemed sufficient to still rule out either a hemorrhage or ischemic lesion; a score of 2 if moderate artifacts were present that allowed for detection of a hemorrhage but not of ischemia; a score of 3 if artifacts were severe and precluded detection of both hemorrhage and ischemia. As there was no significant difference between left and right scores, the two were averaged. Ninety-five percent of scores were in agreement and a consensus review was performed to finalize disagreements about the scores. The images were presented in random order and readers were blinded to the type of scan performed (i.e., circular vs butterfly).

Statistical analysis

As each patient performed both scans (intrapatient control), scores were analyzed using paired Student t-tests. P values <0.05 were considered significant.

RESULTS

We included 94 paired CBCT scans from 47 patients (47 circular scans and 47 dual-axis butterfly scans) in our study (table 1 and

Table 1 Patient demographics (n=47)

Age (years), median (IQR)	72 (62–80)
<65	32 (68%)
>65	15 (32%)
Gender, n	
Female	25 (53%)
Male	22 (47%)
Stroke Side, n	
Left	22 (47%)
Right	17 (36%)
Posterior fossa	7 (15%)
Other	1 (2%)
Stroke Location, n	
MCA	26 (55%)
Vertebro-basilar	8 (17%)
Carotid T	4 (9%)
Tandem occlusion	4 (9%)
Cervical ICA	3 (6%)
MEVO	2 (4%)

online supplemental figure 1). All scans were postprocessed using a motion-artifact correction algorithm (Cancelliere *et al*, accepted *JNIS*). Two patient scans were excluded owing to excessive movement which could not be adequately corrected with the motion artifact correction algorithm. Each scan was given 36 scores for six types of image artifacts in six anatomical regions (Artifacts: (1) beam hardening, (2) undersampling, (3) inhomogeneity, (4) cone-beam artifacts, (5) metallic artifacts, and (6) patient motion; Regions: left and right upper supratentorial; left and right lower supratentorial; and left and right posterior fossa). Scores were based on a 4-point Likert scale (0=none; 1=mild, + hemorrhage and + ischemia

detection; 2=moderate, + hemorrhage and − ischemia detection; 3=severe, − hemorrhage and − ischemia detection). No significant differences were observed between left and right territories and thus those scores were averaged together. The graphs in figure 2 show the whole brain and territory-specific average artifact scores between circular and DA butterfly scans. Average whole brain artifact scores (including the average of all six regions for each scan), showed that the dual-axis butterfly scans had significantly fewer image artifacts than the circular scans (average artifact score ($_{avg}$AS)=0.20 vs 0.33; p<0.001).

Compared with the 10 s circular scans, the 8 s butterfly scans had significantly improved beam hardening ($_{avg}$AS=0.13 (butterfly) vs 0.78 (circular); p<0.001) and almost eliminated cone-beam artifacts ($_{avg}$AS=0.04 (butterfly) vs 0.55 (circular); p<0.001). As expected, the dual-axis butterfly scan did have more undersampling artifacts ($_{avg}$AS=0.40 (butterfly) vs 0.03 (circular); p<0.001) due to the smaller number of acquired images (480 vs 620 images, see Methods). Specific to brain region, beam hardening improved in all regions, with the biggest improvement in the posterior fossa, $_{avg}$AS=1.47 (circular) vs 0.27 (butterfly), p<0.001; and cone-beam artifacts were primarily improved in the upper supratentorial regions, $_{avg}$AS=1.26 (circular) vs 0.10 (butterfly), p<0.001. Figure 3 demonstrates three different patient examples showing improved cone-beam and beam hardening artifacts for dual-axis scans compared with circular scans.

DISCUSSION

In this study, we assessed six types of imaging artifacts from a novel dual-axis CBCT head scan and compared them with those from a circular scan acquired on the same patient. Using a four point scale between 0 (none) and 3 (severe), we identified improved overall image artifacts in the DA scan, with significant improvement in cone-beam and beam hardening artifacts. These improvements were greatest in the upper supratentorial and posterior fossa regions of the brain. This was expected as cone-beam artifacts are formed by the decreased penetration near the
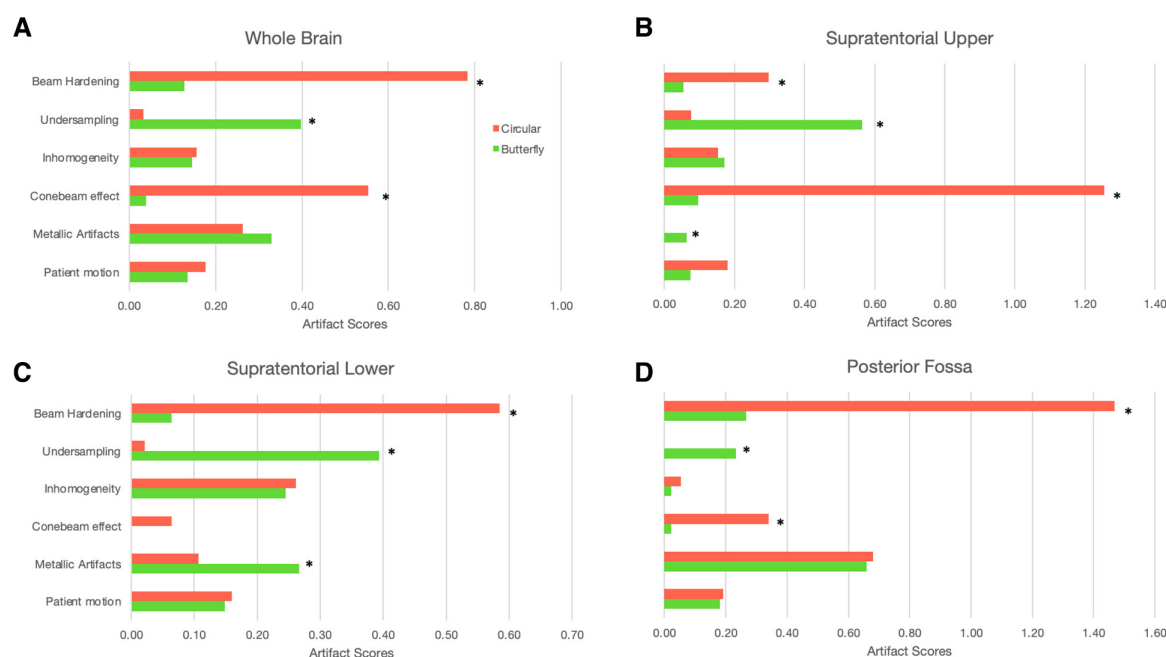

Figure 2 Average artifact scores for 10 s circular versus 8 s butterfly scans for the whole brain (A) and specific brain regions (B–D). Left-side and right-side scores for each region were not significantly different and were therefore averaged together.
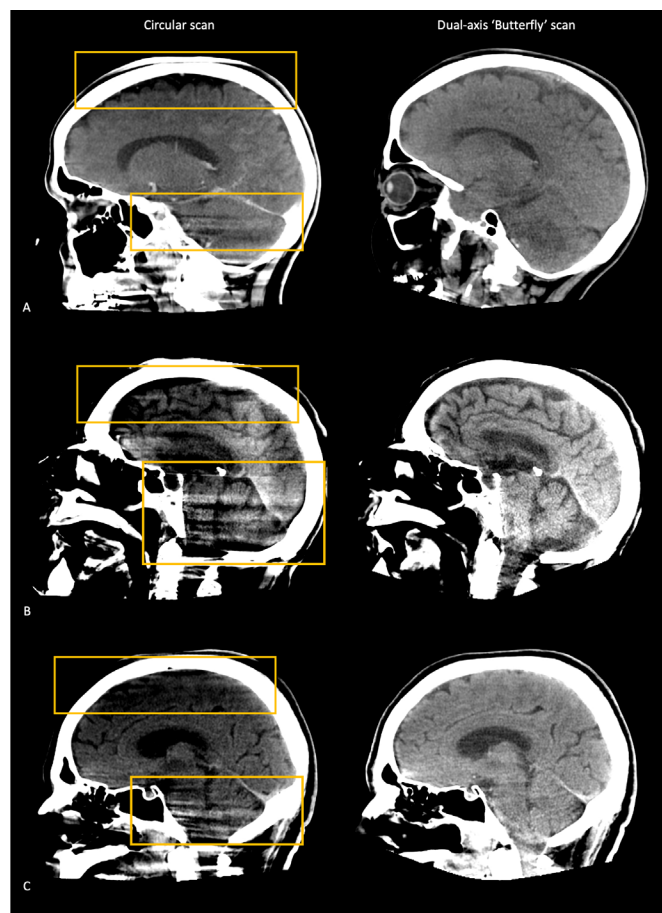
Figure 3 Three patient examples (A–C) demonstrated improved cone-beam (upper yellow square) and beam hardening (lower yellow square) for circular (left) versus dual axis 'butterfly' (right) scans.

outer edges of the X-ray's cone beam, which for a circular scan would occur on the top and bottom of the image. The dual-axis scan was specifically designed to increase penetration at the center of the X-ray beam in these regions by incorporating an X-ray tube trajectory with caudal and cranial angulation. By satisfying Tuy's completeness condition,[12] we were successfully able to improve the cone-beam artifacts and assessment of hemorrhagic and ischemic stroke lesions in these regions, which was previously not possible with the traditional circular scan.

As for the improved bone beam hardening artifacts, we hypothesize that the new path of the dual-axis trajectory avoided scanning through superimposed bony regions which decreased X-ray attenuation and beam hardening along the trajectory. This was prominently observed in the lower supratentorial region where the teeth would traditionally be superimposed over the base of the skull in the circular trajectory scan, resulting in a high X-ray beam attenuation. The dual-axis scan, on the other hand, has a cranial angulation at this point which avoids superimposition of the maxillary region and the base of the skull. This could also explain why our results showed increased metallic artifacts in the lower supratentorial region for the DA scan. Metallic objects in the field of view can cause severe streaking artifacts and scatter due to the high density of the object attenuating the X-ray beam. Beam hardening, partial volume, and aliasing can compound to exacerbate metal artifacts. The new DA trajectory might have moved the direction of streaks, caused by metal dental hardware, from an axial plane through the posterior fossa

to a cranial direction through to the lower supratentorial region for some patients.

These findings further reinforce the teaching point that patient head positioning for CBCT imaging is important in order to minimize the number of image artifacts. For instance, the front to back, left to right, and vertex to base of the skull should all be positioned equidistant from the four edges of the image detector to ensure that the center of the X-ray beam penetrates the skull appropriately. We observed that if the skull is positioned with a left-sided or right-sided offset, increased scatter could cause an inhomogeneity artifact.

It is important to note that the DA scan protocol used in our study had a shorter acquisition time, resulting in fewer acquired images (480 vs 620). This was motivated by improved workflow and intended to decrease the probability of motion artifacts; however, it resulted in significantly more view aliasing artifacts due to insufficient angular sampling, while the difference in motion artifacts was not significant. Therefore, in the future we would recommend incorporating at least 600 images for a CBCT head scan. Future systems could improve workflow by increasing the frame rate. Other types of image artifacts have been described in the literature but may be more prevalent in other types of medical imaging, such as CT or MRI, and are not commonly seen in CBCT imaging and thus were not included in our analysis. For example, windmill artifacts are a type of scanner-based artifact that appear as equally distanced bright streaks diverging from a focal high-density structure. These artifacts are encountered during helical multidetector CT acquisitions and are caused by inadequate data sampling in the z-plane, due to multiple detector rows intersecting the reconstruction plane during each rotation of the gantry.

We have noticed an improvement in overall quality of cone-beam CT over the past few years. First, shorter acquisition times accompanied by higher doses and advanced postprocessing were shown to improve image noise, artifacts, and gray/white matter differentiation for circular scans.[5] Although there have been many improvements since the first maxillofacial examination in 1994, CBCT image quality could be further improved by increasing the radiation dose. The protocols in this study used 45 mGy, which is more than 50% lower than a typical non-contrast CT head scan (~100 mGy). Increasing the dose minimizes photon starvation and improves contrast resolution. Deep learning could also be used to improve image artifacts. Harms *et al*, 2019 used a res-cycle GAN to learn a mapping between CBCT images and paired planning CT images to successfully improve image quality.[20]

As previously mentioned, improved CBCT imaging in the angiosuite supports a direct-to-angio approach for acute ischemic stroke treatment. Bypassing CT or MR and bringing patients with acute ischemic stroke directly to the angiosuite for endovascular thrombectomy can shorten the time to treatment by up to 1 hour,[6] which can significantly improve patient outcomes.[7] Although the benefits for patients are clear, the direct-to-angiosuite approach may increase the number of patients with stroke who are transported to the angiosuite, which in light of the ongoing COVID-19 pandemic, may cause increased potential exposure of the neurointerventional team to the virus.[21–23]

Our study has some limitations. All scans were acquired at a single center, thus a multicenter study is suggested to increase robustness of the study. Additionally, we did not use any quantitative measures to classify artifacts as this method would be extremely tedious and subject to error if performed manually, particularly as these quantities change depending on the multiplanar reformat (axial vs coronal vs sagittal). If, however, it could be objectively and efficiently measured

using an automated artifact classification tool, quantitative measures could be considered.

There is still controversy about how much information from imaging is needed to justify proceeding with mechanical thrombectomy treatment. Additional imaging comes with the cost of time, and the clinical trials have repeatedly shown that time is an independent predictor of a patient's outcome.[7] We look forward to the results of the ongoing WE-TRUST trial (Workflow Optimization to Reduce Time to Endovascular Reperfusion for Ultra-fast Stroke Treatment; ClinicalTrials.gov Identifier: NCT04701684) which will randomize patients with stroke to direct-to-angio versus CT-first to unbiasedly understand the cost versus benefit of this approach.

CONCLUSIONS

Acute ischemic stroke caused by a large vessel occlusion can be fatal if patients are not treated quickly and effectively. Bypassing CT in a 'direct-to-angio' approach can significantly reduce door-to-puncture times within hospitals and improve patient outcomes. However, brain imaging has an important role for patient selection and to rule out hemorrhage. To date, cone-beam CT imaging can be acquired in the angiosuite, but its image quality is inferior to that of CT, making brain parenchyma assessment more challenging. Identification and correction of CBCT image artifacts will facilitate the development of new scans with improved image quality that enable selection of patients with AIS.

Our study shows that a novel dual-axis 'butterfly' cone-beam CT trajectory nearly abolishes cone-beam artifacts and significantly improves bone beam hardening artifacts in comparison with circular CBCT scans. These improvements suggest that CBCT image quality may be sufficient for selection of patients with AIS and support a direct-to-angiography treatment workflow in the future.

ORCID iDs
Nicole Mariantonia Cancelliere http://orcid.org/0000-0002-8703-4304
Fred van Nijnatten http://orcid.org/0000-0001-6108-2255

REFERENCES

1 Eckert M, Gölitz P, Lücking H, et al. Optimized flat-detector CT in stroke imaging: ready for first-line use? *Cerebrovasc Dis* 2017;43:9–16.
2 Xu J, Sisniega A, Zbijewski W, et al. Technical assessment of a prototype cone-beam CT system for imaging of acute intracranial hemorrhage. *Med Phys* 2016;43:5745–57.
3 Leyhe JR, Tsogkas I, Hesse AC, et al. Latest generation of flat detector CT as a peri-interventional diagnostic tool: a comparative study with multidetector CT. *J Neurointerv Surg* 2017;9:1253–7.
4 Maier IL, Leyhe JR, Tsogkas I, et al. Diagnosing early ischemic changes with the latest-generation flat detector CT: a comparative study with multidetector CT. *AJNR Am J Neuroradiol* 2018;39:881–6.
5 Nicholson P, Cancelliere NM, Bracken J, et al. Novel flat-panel cone-beam CT compared to multi-detector CT for assessment of acute ischemic stroke: a prospective study. *Eur J Radiol* 2021;138:109645.
6 Psychogios M-N, Behme D, Schregel K, et al. One-stop management of acute stroke patients: minimizing door-to-reperfusion times. *Stroke* 2017;48:3152–5.
7 Bourcier R, Goyal M, Liebeskind DS, et al. Association of time from stroke onset to groin puncture with quality of reperfusion after mechanical thrombectomy: a meta-analysis of individual patient data from 7 randomized clinical trials. *JAMA Neurol* 2019;76:405–11.
8 Wu P, Sisniega A, Stayman JW, et al. Cone-beam CT for imaging of the head/brain: development and assessment of scanner prototype and reconstruction algorithms. *Med Phys* 2020;47:2392–407.
9 Sisniega A, Zbijewski W, Xu J, et al. High-fidelity artifact correction for cone-beam CT imaging of the brain. *Phys Med Biol* 2015;60:1415–39.
10 Barrett JF, Keat N. Artifacts in CT: recognition and avoidance. *Radiographics* 2004;24:1679–91.
11 Nagarajappa AK, Dwivedi N, Tiwari R. Artifacts: the downturn of CBCT image. *J Int Soc Prev Community Dent* 2015;5:440–5.
12 Tuy HK. An inversion formula for cone-beam reconstruction. *SIAM J Appl Math* 1983;43:546–52.
13 Schomberg H. Complete source trajectories for C-arm systems and a method for coping with truncated cone-beam projections. Proc Sixth International Meeting on Fully Three-Dimensional Image Reconstruction in Radiology and Nuclear Medicine, 2001:221–4.
14 Jiang X. *Patient radiation dose when using XperCT and rotational X-ray*, 2013. https://espace.library.uq.edu.au/view/UQ:f69994b
15 Wang C, Nguyen G, Toncheva G, et al. Evaluation of patient effective dose of neurovascular imaging protocols for C-arm cone-beam CT. *AJR Am J Roentgenol* 2014;202:1072–7.
16 Schomberg H. A Fourier-filtered backprojection algorithm for cone-beam CT. Proc 8th International Meeting on Fully Three-Dimensional Image Reconstruction in Radiology and Nuclear Medicine, 2005:184–8.
17 Joseph PM, Spital RD. A method for correcting bone induced artifacts in computed tomography scanners. *J Comput Assist Tomogr* 1978;2:100–8.
18 Kijewski PK, Bjärngard BE. Correction for beam hardening in computed tomography. *Med Phys* 1978;5:209–14.
19 Nalcioglu O, Lou RY. Post-reconstruction method for beam hardening in computerised tomography. *Phys Med Biol* 1979;24:330–41.
20 Harms J, Lei Y, Wang T, et al. Paired cycle-GAN-based image correction for quantitative cone-beam computed tomography. *Med Phys* 2019;46:3998–4009.
21 Aggour M, White P, Kulcsar Z, et al. European Society of Minimally Invasive Neurological Therapy (ESMINT) recommendations for optimal interventional neurovascular management in the COVID-19 era. *J Neurointerv Surg* 2020;12:542–4.
22 Fiorella D, Fargen KM, Leslie-Mazwi TM, et al. Neurointervention for emergent large vessel occlusion during the COVID-19 pandemic. *J Neurointerv Surg* 2020;12:537–9.
23 Fraser JF, Arthur AS, Chen M, et al. Society of NeuroInterventional Surgery recommendations for the care of emergent neurointerventional patients in the setting of COVID-19. *J Neurointerv Surg* 2020;12:539–41.